the plant journal

SEB SOCIETY FOR EXPERIMENTAL BIOLOGY

The Plant Journal (2021) **108,** 303–313 doi: 10.1111/tpj.15511

TECHNICAL ADVANCE

Real-time tracking of root hair nucleus morphodynamics using a microfluidic approach

Gaurav Singh[1,*,†], David Pereira[2,†], Stéphanie Baudrey[3], Elise Hoffmann[1], Michael Ryckelynck[3], Atef Asnacios[2] and Marie-Edith Chabouté[1,*]

[1]*Institut de biologie moléculaire des plantes, CNRS, Université de Strasbourg, Strasbourg 67084, France,*
[2]*Laboratoire Matière et Systèmes Complexes, UMR 7057, CNRS et Université de Paris, Paris 75013, France, and*
[3]*Université de Strasbourg, CNRS, Architecture et Réactivité de l'ARN, UPR 9002, Strasbourg 67000, France*

Received 8 June 2021; revised 6 September 2021; accepted 13 September 2021; published online 25 September 2021.
*For correspondence (e-mails marie-edith.chaboute@ibmp-cnrs.unistra.fr; gaurav.singh@ibmp-cnrs.unistra.fr).
†These authors contributed equally to this work.

SUMMARY

Root hairs (RHs) are tubular extensions of root epidermal cells that favour nutrient uptake and microbe interactions. RHs show a fast apical growth, constituting a unique single cell model system for analysing cellular morphodynamics. In this context, live cell imaging using microfluidics recently developed to analyze root development is appealing, although high-resolution imaging is still lacking to enable an investigation of the accurate spatiotemporal morphodynamics of organelles. Here, we provide a powerful coverslip based microfluidic device (CMD) that enables us to capture high resolution confocal imaging of Arabidopsis RH development with real-time monitoring of nuclear movement and shape changes. To validate the setup, we confirmed the typical RH growth rates and the mean nuclear positioning previously reported with classical methods. Moreover, to illustrate the possibilities offered by the CMD, we have compared the real-time variations in the circularity, area and aspect ratio of nuclei moving in growing and mature RHs. Interestingly, we observed higher aspect ratios in the nuclei of mature RHs, correlating with higher speeds of nuclear migration. This observation opens the way for further investigations of the effect of mechanical constraints on nuclear shape changes during RH growth and nuclear migration and its role in RH and plant development.

Keywords: *Arabidopsis thaliana*, live cell imaging, microfluidics, nucleus, root hair, single cell, technical advance.

Linked article: This paper is the subject of a Research Highlight article. To view this Research Highlight article visit https://doi.org/10.1111/tpj.15534.

INTRODUCTION

Plant developmental programs have largely been investigated at the organ, tissue or whole plant seedling levels, but are increasingly being studied at the single cell level using root hairs (RHs), pollen tubes or isolated protoplasts in Arabidopsis, soybean and maize (Agudelo et al., 2012; Libault et al., 2010; Misra et al., 2019; Qiao et al., 2017; Ryu et al., 2019; Satterlee et al., 2021). The RH is a single differentiated cell from the epidermis that directly interacts with the external environment. RHs are unicellular lateral extensions of root epidermal cells (trichoblast) and display distinct properties concerning cell size, vacuole size and cell surface features (Grierson et al., 2014). RH development occurs in three well defined steps: initiation with outgrowth from a trichoblast cell, elongation via tip growth and maturation when the tip stops growing.

At the molecular level, RH growth is a highly regulated process that is well characterized at the transcriptomic and proteomic levels, notably in soybean (Brechenmacher et al., 2012; Libault et al., 2010). In Arabidopsis, RH specific genes and proteins have been identified as being important for RH development (Lan et al., 2013; Li and Lan, 2015; Petricka et al., 2012). Indeed, a spatiotemporal gene expression controls RH growth (Shibata et al., 2018; Yi et al., 2010).

At the cellular level, RHs comprise tubular structures of 10 μm in diameter that elongate uniaxially, perpendicular to the main root axis, and can reach 1 mm in length (Grierson et al., 2014). RH hair development is tightly controlled by cytoskeleton reorganization and vesicle trafficking controlled

by the small Rho GTPases (Jones et al., 2002; Kang et al., 2017; Ketelaar et al., 2002; Krupinski et al., 2016). Tip growth involves trafficking of secretory and endocytic vesicles providing building blocks for the cell wall and plasma membrane in the cytoplasmic dense area (Hepler et al., 2001; Ketelaar et al., 2002). A cortical cytoplasm surrounds a vacuole that ensures turgor pressure needed for RH growth (Volgger et al., 2010). RH growth shows variation in its rate with an early growth rate of 0.4 μm min^{-1} (i.e. until RH protrusion reached a size of 20–40 μm and a late growth rate of 1–2.5 μm min^{-1}) (Dolan et al., 1994). During RH growth, the nucleus is at a mean distance of 77 $\pm$ 15 μm from the tip (Ketelaar et al., 2002). In mature RHs with stopped growth, a basipetal movement of the nucleus occurs randomly with intervals of pausing (Chytilova et al., 2000).

A few studies have shown that nuclear migration in the RH may be associated with various cellular responses against environmental stimuli, including symbiosis, plant microbe interaction, nutrient and water uptake, as well as response to light (Griffis et al., 2014; Tamura et al., 2013). During RH growth, the nucleus position and movement appear to be tightly regulated. At least in Arabidopsis, they are notably controlled by actin and its associated proteins myosin XI-i (Ketelaar et al., 2002; Tamura et al., 2013), with the migration direction of RH nuclei being closely related to the perinuclear actin filaments (Zhang et al., 2019).

During RH growth, the nucleus is also reported to change its shape (Chytilova et al., 2000). However, no clear correlation between nuclear movement and nuclear shape changes has been established. Investigating such a link between nuclear shape changes and nuclear movement during development would be of great interest with respect to understanding the role of mechanotransduction in plant growth. Indeed, changes in nuclear shape were recently correlated with the induction of stress responsive and developmental genes during organogenesis in Arabidopsis (Fal et al., 2021; Landrein et al., 2015) and plant adaptation to their environment (Goswami, Asnacios, Hamant et al., 2020; Goswami, Asnacios, Milani et al., 2020).

Thus, to investigate the link between RH growth, nuclear movements and shape changes, we have developed a simple microfluidic platform coupled with high resolution microscopy to monitor nuclear shape and movements during RH development in real time and in a controlled and standardized environment. First, to validate this new coverslip based microfluidic device (CMD), we measured various parameters of RH growth that are well documented in the literature, such as RH velocity and mean nuclear position with respect to RH tip. In addition, as an illustration of the new possibilities offered by the CMD, we report accurate descriptions of nuclear shape changes during RH growth, as well as a significant difference in the nuclear aspect ratio that correlates with a difference in migration speeds for nuclei observed in growing and mature RHs.

RESULTS

Experimental setup of the coverslip based microfluidic device for RH growth

To visualize RH growth and nucleus dynamics, we developed a CMD chip to track and image RHs in real time under confocal microscopy. The devices were made up of polydimethylsiloxane (PDMS), an elastomer that was covalently bound to a microscope glass coverslip. Each chip consisted of three independent devices, allowing one to grow three individual Arabidopsis seedlings in independent main channels under a constant flow of ½ MS liquid media supplemented with sucrose (see Materials and methods). The seedlings were added into the chip prefilled with the media. To avoid crossed contamination between the channels, three independent input and output ports were used. Plantlets were germinated on ½ MS agar media in tips that were transferred to the PDMS chip at 1 cm from the media input point and at a 45° angle with respect to the device (Figure 1a,b, Figure S1a). Each device was made of three parallel 1.5 cm-long channels connected via two arrays of lateral 400 μm-long perpendicular channels (Figure 1b, Figure S1b). The main central channel is used for root growth, with two lateral channels for media supply and small connecting channels for RH growth. The total volume of the chamber was 6 μl. The root growth was under a constant flow rate (8 μl min^{-1}) in ½ MS liquid media supplemented with sucrose (see Materials and methods). The device has a 250 μm-width and 100 μm-depth channel for main root growth (Massalha et al., 2017) (indicated in light and dark blue, respectively, in Figure 1b) and 20 μm-width and-depth lateral channels for RH expansion (indicated in red in Figure 1b, Figure S1b). After 4–5 days, a main root of approximately 12 mm in length could be observed in each device (Figure 1c) and the device remained functional until the main root reached the end of the main channel, after approximately 8 days. Under a microscope, the device was subjected to a continuous flow rate of liquid media, and RH growth could be monitored under controlled conditions at high resolution. If needed, the medium could be replaced in approximately 30 sec using a transient flow rate of 1000 μl min^{-1}, with lateral channels being filled simultaneously all along the chip (Figure S2 and Movie S1).

Accurate investigation of RH growth dynamics using CMD

The RH is a differentiated cell that displays a tubular structure protruding from the surface of the root trichoblast cell. It is characterized by a polarized structure and tip expansion. The rate of RH growth has been already well described in Arabidopsis (Dolan et al., 1994). To validate our microfluidic system, we measured this parameter by following growing RH for 60 min using confocal microscopy (Figure 2a, Movie S2). The tip position of 29

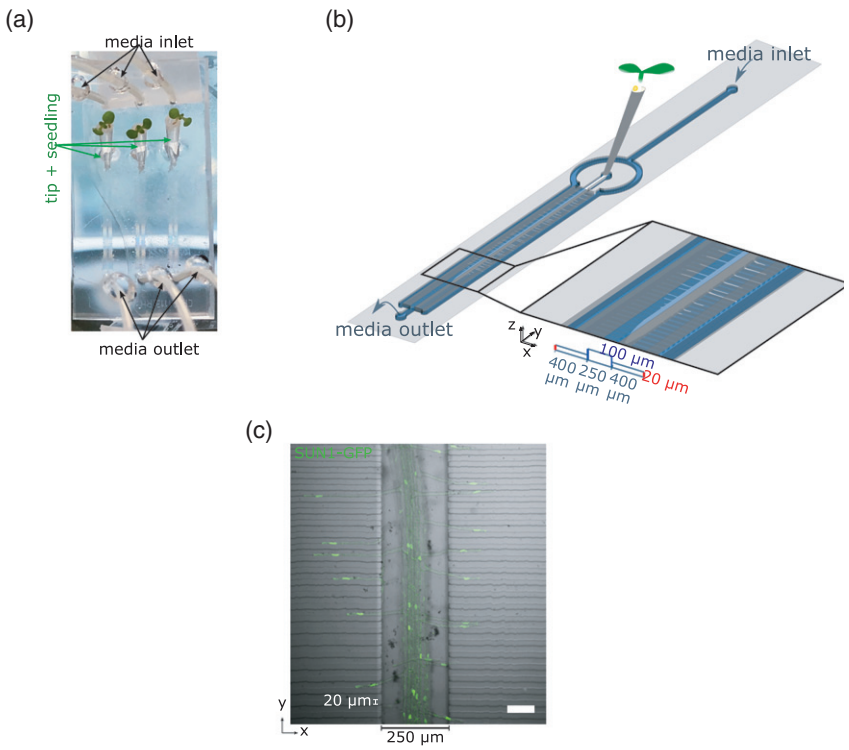

Figure 1. Experimental procedures and the coverslip based microfluidic device (CMD) chip details for root hair (RH) analysis.
(a) Top view of 9-day-old Arabidopsis seedlings growing in a micropipette tip, filled with ½ MS media. Tips were inserted in a CMD chip. (b) A schematic 3D diagram of the CMD design with the illustration of root and RH in the main and side channels, respectively. Light blue colour indicates the width of the main channel and the length of the lateral channels. The depth of the main and lateral channels is indicated in blue and red, respectively. (c) A 10× magnification image of root grown in the CMD with RH expanding in the lateral channels. Plantlets expressing the nuclear envelope marker SUN1-GFP were used here, with fluorescence images highlighting the root. RH and nuclei were merged with differential interference contrast visualization of the PDMS chip (Scale bar = 100 µm).

individual RHs was a linear function of time, indicating a constant growth speed. To evaluate the speed of growth of each individual cell, each curve was fitted independently with a linear model. The distribution of growth speeds had a median value around 1.5 ± 0.3 µm min^{-1} (Figure 2b,c). This result fits perfectly with the data of Dolan et al. (1994) who describe a growth rate of between 1 and 2.5 µm min^{-1}. Thus, our microfluidic device is suitable for the growth and investigation of Arabidopsis RH cells.

Migration of individual nuclei in growing RH

RH tip growth and migration of the nucleus are highly inter-dependent processes (Ketelaar et al., 2002). To monitor the nuclear migration in the growing RH tube, we followed the dynamics of individual nuclei during 16 min by acquiring Z-stack images every 2 min via confocal microscopy. We used seedlings expressing a nuclear envelope marker (SUN2-RFP) (Tamura et al., 2013) in the Col-0 GFP-MBD line (Camilleri et al., 2002). Moreover, we concomitantly analyzed the movement of the nucleus and the tip growth in two individual RH (Figure 3a). A kymograph analysis of the cell periphery (bright field) and nuclear envelope signals (Figure 3b) showed that the growth of the RH tip (grey) and the movement of its nucleus (red) evolved similarly. This was confirmed through the evaluation of the positions of the nucleus (red curves) and tip (blue curves) (Figure 3c), where nucleus migration and tip growth showed parallel curves with quite similar speeds (cell 1: Vtip1 = 1.6 µm min^{-1}, Vnuc1 = 2.1 µm min^{-1}; cell 2: Vtip2 = 1.7 µm min^{-1}, Vnuc2 = 1.3 µm min^{-1}). This was also demonstrated through the evaluation of the distance between the nucleus and the tip (d_{n-t}), which remains more or less constant over time (Figure 3d and Figure S3, Movie S3) during tip growth. The mean speed of the nucleus in the growing RH was 2.3 ± 0.6 µm min^{-1} (n = 10). Of note, observations at long time scales (Figure S4) show that the rate of RH tip growth is quite constant, whereas the speed of nucleus displacement can display noticeable fluctuations around its mean value. Thus, although the mean distance between the nucleus and the RH tip is conserved during growth, the nucleus may go back-and-forth around its mean position (Figure S3) as described previously (Zhang et al., 2019).

When the RH stopped its growth, the nucleus lost its conserved position from the RH tip and was located randomly in the RH, also showing back-and-forth movement. In mature RHs (n = 28), nuclear movement occurs over very short distances (10% of nuclei) or over long distances (90% of nuclei). Interestingly in the latter case, the velocities of nuclei were quite similar, with mean speeds of 4.1 ± 0.6 µm min^{-1} (n = 10) and 3.2 ± 1.7 µm min^{-1} (n = 6) for the backward and forward movements, respectively. In addition, the nucleus changed its shape (Movie S4). Such nuclei velocities may be consistent with previously reported data obtained using classical approaches (analyses of RH growth in 0.5% phytagel)

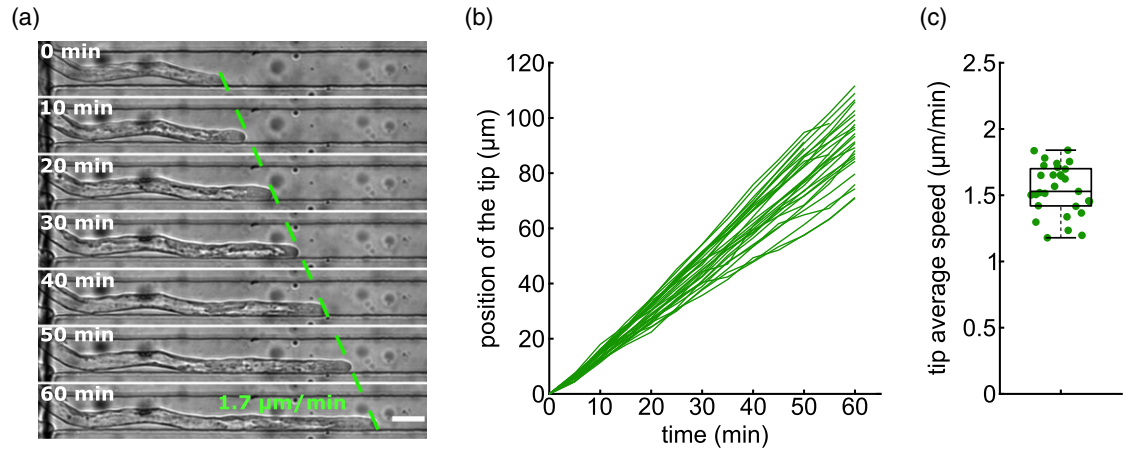

Figure 2. Arabidopsis root hair (RH) tip growth in real time.
(a) Bright field sequential images from a time-lapse recording of *Arabidopsis* growing RH to follow the tip growth. Images were taken every min (Movie S2) but presented here at only 10-min intervals. (b) Growth curves of individual RH (n = 29). (c) The distribution of the average speeds of the growing RH has a median of 1.5 µm min^{-1}. Live imaging was recorded using 10× magnification (n = 29, scale bar = 20 µm).

where time lapse imaging was less resolutive (Chytilova et al., 2000; Van Bruaene et al., 2003). Thus, our device is shown to be suitable for precisely imaging the positioning and dynamics of the nucleus in RH cells, at the same time as preserving the characteristics observed with more usual growing methods.

Real-time fluctuations of the nuclear shape in growing RHs

Fluctuations of the nucleus shape under different conditions have been well studied in metazoans (Chu et al., 2017; Dorland et al., 2019; Versaevel et al., 2012) but less so in plant systems. To investigate the nuclear shape fluctuations in real time, SUN1-GFP expressing RH cells (Graumann et al., 2010) were scanned in CMD chips for 10 min, with Z-stacks performed every 1 min. The nucleus can undergo quick and significant deformations (Figure 4a and Figure S5) (n = 12) as shown by the evaluation of the nuclear aspect ratio, which is defined as the ratio between the nuclear lengths that are parallel and perpendicular, respectively, to the RH axis. Indeed, in the example presented in Figure 4, the aspect ratio of the nucleus increased by 38% in 2 min (from 2.1 to 2.9) and decreased by 32% after an additional 4 min (from 2.9 to 1.9), which was consistent with the circularity measurement (Figure 4b). During the same period, the nuclear projected area decreased by 26%. By contrast, the apparent perimeter did not appear to be affected by the shape changes. This 2D shape analysis is of course partial because the nucleus is a 3D structure. 3D reconstructions of the nucleus showed that the nuclear shape indeed changed during RH growth and nucleus movement (Figure 4c), confirming the conclusions obtained from 2D projections. The same type of quick and significant deformations described previously in 2D can also be observed in the y–z plane showing transverse section view (Figure 4d). Remarkably, these images revealed the uneven shape of the nucleus. Conversely, from this analysis, it appears that the nucleus volume is quite constant during nucleus movement and deformations (Figure 4e). Altogether, these results show that the nucleus of RH cell is a highly dynamic structure that undergoes significant 3D shape deformations.

Comparing nuclear positions and shapes in growing and mature RHs

Previous studies have reported that nuclear position is RH stage dependent (Ketelaar et al., 2002). To verify this result under our controlled and standardized conditions, we monitored nuclei in growing and mature RH cells (Figure 5a). The quantification of the nucleus to tip distance d_{n-t} in the two phases shows that the nucleus is closer to the RH tip during the growing phase (median value 85 ± 20 µm) than in the mature phase (median value 232 ± 101 µm) (Figure 5b). Of note, the distribution of the d_{n-t} is larger for mature compared to growing RHs. These results are in good agreement with the literature (Ketelaar et al., 2002). Interestingly, the nuclear projected area is not affected by the stage of the RH (Figure 5c). By contrast, the nuclear aspect ratio was notably affected by the RH stage. Indeed, values of the average aspect ratio of nuclei were 3.18 ± 1.57 and 5.72 ± 1.80 in growing (n = 38) and mature (n = 35) RHs, respectively (Figure 5d). This indicates that the nucleus aspect ratio increased by 45% in the mature phase compared to growing RHs.

DISCUSSION

Here, we present a microfluidic approach for following the dynamics of RH development, placing more emphasis on

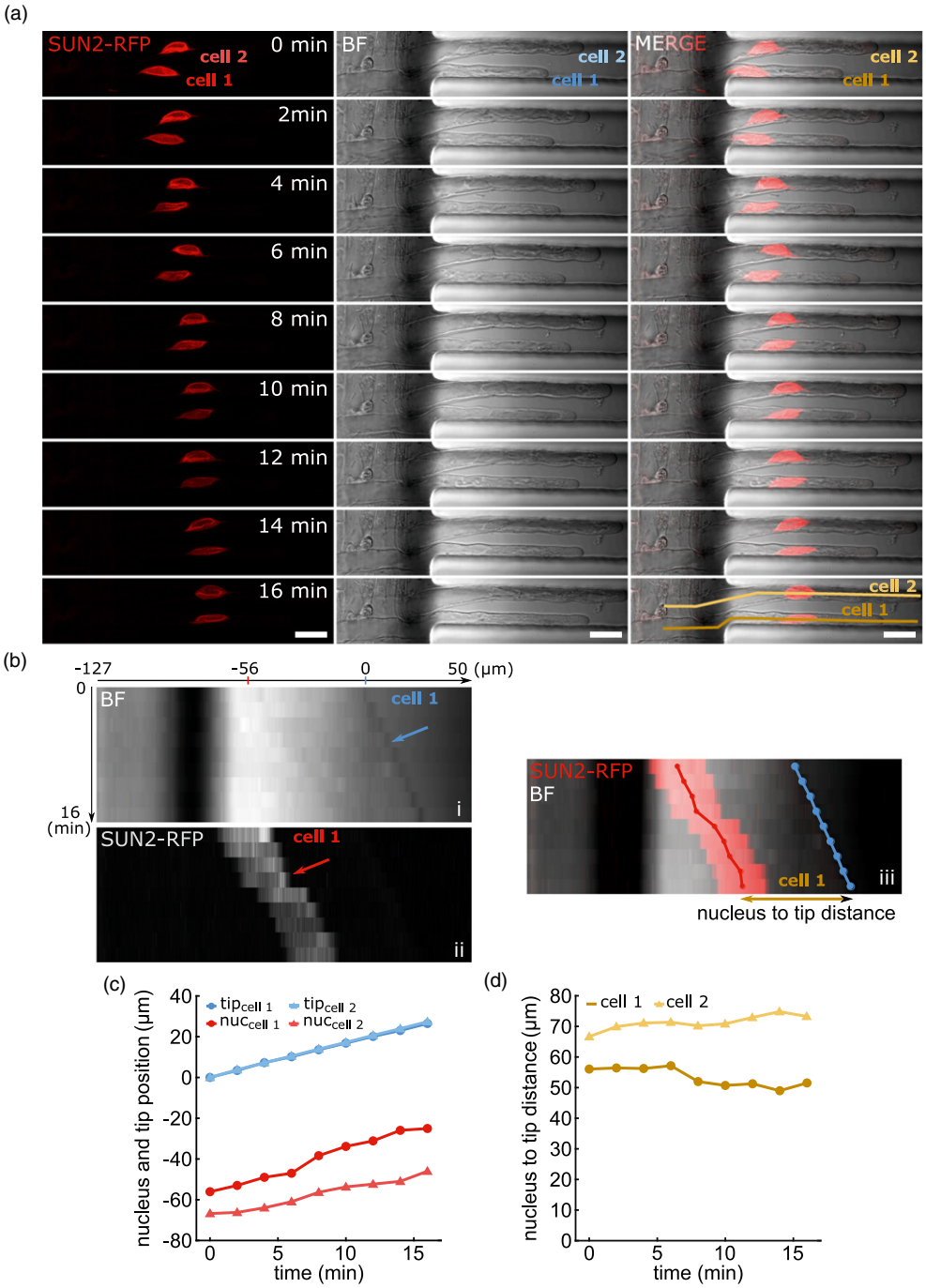

Figure 3. Nuclear migration in growing root hair (RH) of an Arabidopsis line expressing the SUN2-RFP nuclear envelope marker.
(a) Nucleus (in red) maintains a fixed position compared to the RH tip (in grey). Time lapse over 16 min and Z-stack (1 μm, 21 slides, part of the Movie S3) recording of two RH presented here as a sum slices projection at 2-min intervals. Brown and yellow lines: lines over which the positions of the nuclei and RH tip over time were determined for cells 1 and 2, respectively. These positions were used to obtain kymographs of (b), with curves in (c) and (d) indicating the trajectories followed by nuclei 1 and 2 in their respective cells. (b) Kymographical representation of RH tip (top) and nuclear (bottom) positions in a growing RH (cell 1). (c, d) Graphical representation of nuclear (red) and tip position (blue) during RH growth. The distance between nucleus and RH tip was evaluated (yellow). Circles and triangles are for cells 1 and 2, respectively. Scale bar = 20 μm.

nuclear shape changes with high resolution microscopy. As a validation of the technique, we show that both RH growth and nuclear migration display characteristics similar to those previously obtained using more conventional methods (Dolan et al., 1994; Ketelaar et al., 2002). Here, we are able to accurately describe, in time and space,

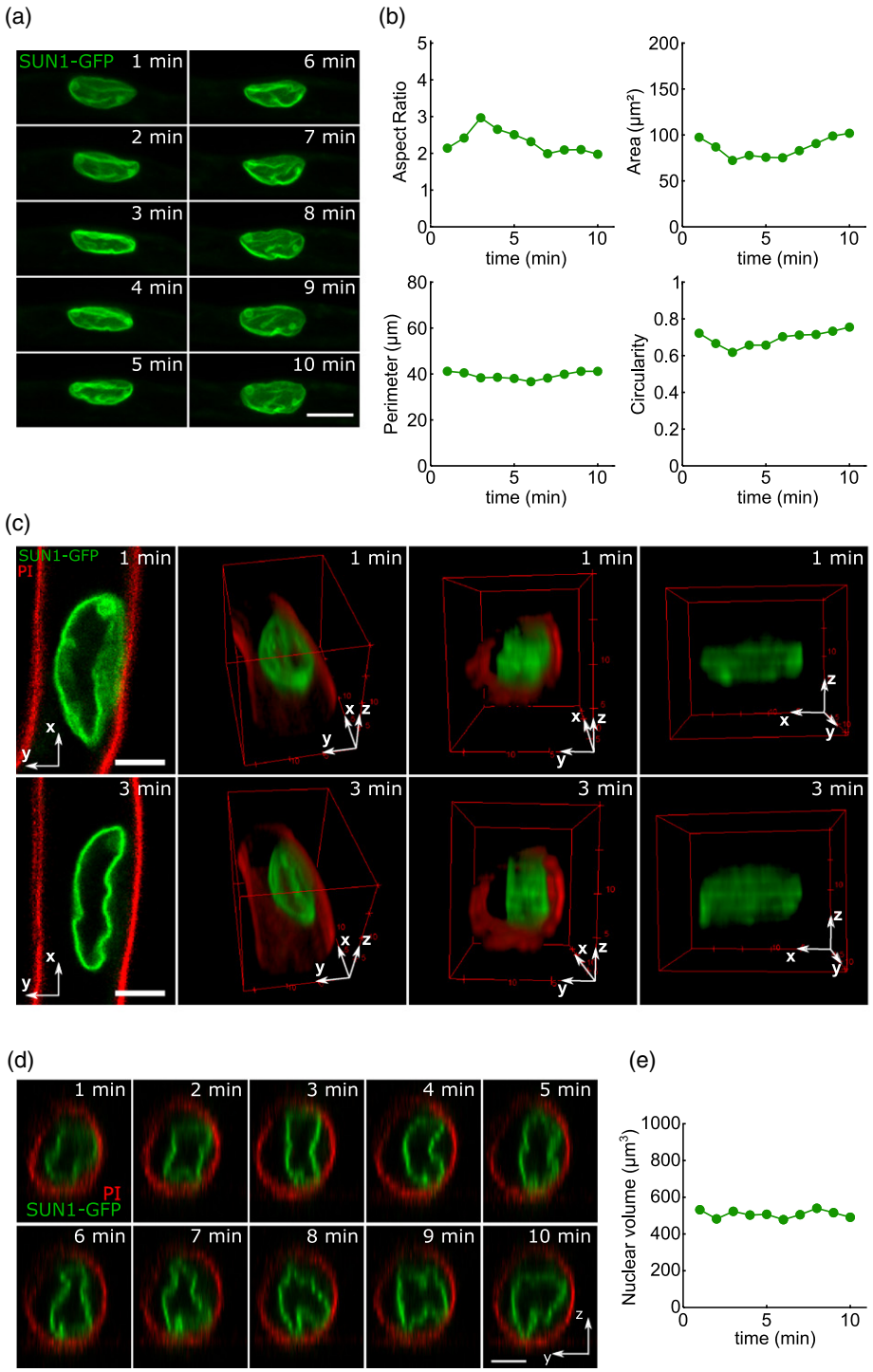

Figure 4. *In vivo* time-laps imaging showing fluctuations in the nuclear shape of a growing root hair (RH) in real time.
(a) Ten-minute sequence of time lapse recording of *SUN1-GFP* RH nucleus. Z-stacked images are presented (sum slices projection). Pictures were taken every 1 min. (b) Analysis of nuclear shape fluctuation in real time, presenting aspect ratio, nuclear area, perimeter and circularity. These 2D parameters were determined in a typical interval of 5% of the measured value (scale bar = 10 μm). Measurements for other RH nuclei are provided in Figure S5. (c) Focus on 3D shape changes. The left column displays the 2D section of the nucleus undergoing the most important shape change over 2 min. The three remaining columns display 3D reconstructions of the nucleus in different views. Propidium iodide staining (in red) reveals the RH cell wall. (d) Transverse section view (*y*–*z* plane) showing nuclear shape changes over time. (e) Nuclear volume as a function of time. Nuclear volumes estimated from Z-stacks were determined in a typical interval of 20% of the measured value (scale bar = 5 μm).

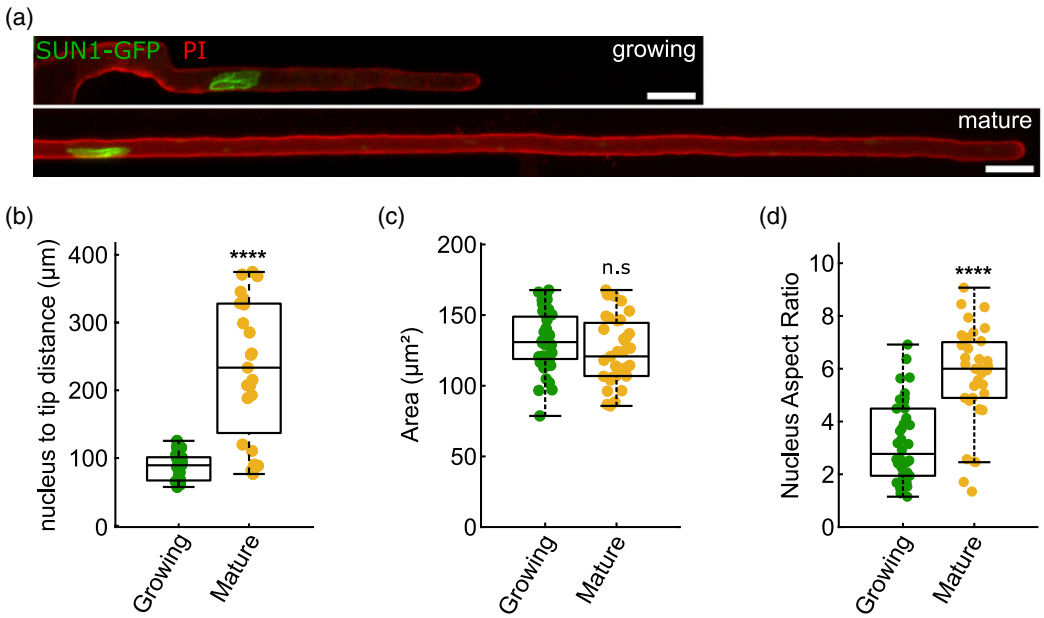

Figure 5. Comparison of the positions and shapes of growing and mature root hair (RH) nuclei.
(a) Representative images of the position of the nucleus during the growing and mature phases (propidium iodide in red, SUN1-GFP in green; scale bar = 20 µm). (b) Quantification of the distance between the nucleus and the tip for growing and mature RH cells (n = 23). (c, d) Quantification of the nuclear projected area (c) and the nucleus aspect ratio (d) of growing (n = 38) and mature (n = 35) RH (t-test; ****$P < 0.0001$).

the highly dynamic behaviour and migration of the nucleus not only during RH growth, but also after growth termination with, for example, significant changes in nuclear aspect ratio.

Microfluidic approaches are just emerging in plants. They have been used to follow root growth and gene expression under various growth conditions (Busch et al., 2012; Fendrych et al., 2018; Guichard et al., 2020) for phenotyping (Jiang et al., 2014) or to track root interaction with pathogens (Massalha et al., 2017; Parashar and Pandey, 2011). Single cell analysis was also developed to follow protoplast development (divisions and growth) (Massalha et al., 2017) or RH growth analysis. RH morphology was evaluated and quantified in response to environmental stresses (Aufrecht et al., 2017) such as hormones (Sun et al., 2021) or phosphate supply (Stanley et al., 2018) using microfluidics. At the subcellular level, only movement of organelles (Golgi, peroxisomes and mitochondria) was evaluated during a short time scale (Aufrecht et al., 2017). Accordingly, the present study enables insights into subcellular imaging, showing a deep analysis of nuclear shaping during RH development. The CMD chip reported here provides a very easy and robust platform for investigating, in real time and at high resolution, nuclei morphodynamics during RH development under controlled conditions.

RH growth is very dynamic in Arabidopsis and may vary from 1 to ~2.5 µm min^{-1} (Wymer et al., 1997). Our real-time RH tip growth rate analysis also showed similar results. During RH growth, we observed a polar migration of the nucleus coordinated with the tip growth as described previously (Vassileva et al., 2005). Although microtubules guide RH tip growth (Sieberer et al., 2005), the nuclear movement has mainly been described, up to now, as actin-myosin XI-i dependent in Arabidopsis (Tamura et al., 2013; Zhang et al., 2019). Beyond RH development, nuclear migration is also involved in various biological processes, such as polar growth of the pollen tube or the responses to mechanical stimuli (Griffis et al., 2014). Interestingly in Arabidopsis, impaired nuclear lamina KAKU4 affects the nuclear shape of the vegetative nuclei and their orderly migration with sperm cells in pollen tubes (Goto et al., 2020). In tobacco BY2 cells, nuclear migration was observed from the cell periphery to the cell centre after protoplast regeneration when the cell axis was induced. However such nuclear migration was delayed when either KCH kinesins, as microtubule-actin filament cross-linkers, or histone H2B are mis-expressed (Brochhausen et al., 2016). Nuclear migration defects were also observed during apical growth in *Physcomitrella* defective for the KCH kinesins (Yamada and Goshima, 2018).

During nuclear migration, a pulsatile RH growth kinetics was described (Wymer et al., 1997) and this could be in agreement with the dynamic changes of nuclear shape that we observed in our microfluidic system. Even though changes in nuclear shape have already been described (Chytilova et al., 2000), these were not analyzed in depth.

In the fully expanded root RH (i.e. mature RHs with no more growth), rapid movements of the nuclei (4–5 μm min^{-1}) over long distances have been described previously (Chytilova et al., 2000) and were also found in our analyses. This apical and basal nuclear movement is a random process and its amplitude may vary with the time. In our experiments, although nuclear area did not change significantly between growing and mature RHs, the aspect ratio of the nuclei increased by a factor of 1.8 in mature RHs. Interestingly, this nuclear shape change correlated with the speed of nuclear movement, which was also increased in the same proportions ($\times$1.6) in mature RHs. This correlation could be of importance for RHs with respect to their development and should be investigated further. Indeed, the increase of the nucleus aspect ratio could be interpreted as a consequence of the fast movement of the nucleus in a dense cytoplasmic environment. For example, a nucleus strongly pulled by cytoskeleton components might deform as a result of the drag exerted by the surrounding cytoplasmic material. The question would then be to determine whether RH maturation is accompanied by an increased speed of nuclear movement leading to higher drag and increased nuclear deformation (which may lead to modified gene expression) or, conversely, whether RH growth arrest is concomitant with a modification of the nuclear structure that leads to a more deformable nucleus offering less resistance to drag and higher speeds of displacement.

Indeed, when components of the nuclear envelope (such as the LINC complexes WIP/WIT, SUN) or of the nucleoskeleton (KAKU4, CRWN1) are affected, the nuclei lose their potency to elongate in RHs (Meier et al., 2016). Interestingly, changes in nuclear shape may also be related to the speed of RH growth (Newman-Griffis et al., 2019) and in turn to changes in RH tip cell wall viscosity, which is one of the main parameters controlling the rate of plant cell elongation (Lockhart, 1965). We cannot exclude the possibility that those changes in nuclear shape may result from chromatin dynamics linked to transcriptional programs occurring during RH growth. In human cells, fluctuation in the nuclear shape is driven by thermal and active processes, caused by the physical forces generated by cytoskeleton and chromatin dynamics that not only affect gene regulation, but also contribute to high rates of nuclear import and export (Almonacid et al., 2019; Chu et al., 2017). The nuclear aspect ratio was also shown to increase with microtubule stabilization in animals (Balakrishnan et al., 2020) and this could also be correlated with less, but more stable, microtubules in mature RHs (Van Bruaene et al., 2004; Vassileva et al., 2005).

In conclusion, using a CMD chip, we have investigated nuclear dynamics at high temporal and spatial resolutions and also questioned the importance of nuclear fluctuation in RH development. Such information would have been extremely difficult to access without the use of our device. This opens the way for understanding the fine tuning of the molecular and biophysical processes behind the nuclear shape changes in response to environmental stresses. Our system opens up new avenues to provide, at the subcellular level, data more amenable for mathematical modelling, with a focus on the nuclear envelope, chromatin and cytoskeleton dynamics. Altogether, we anticipate that our CMD will provide a unique tool for investigating subcellular morphodynamics via high resolution imaging with respect to mechanotransduction in root and plant development, and, more generally, the sensitivity of RHs to environmental conditions.

EXPERIMENTAL PROCEDURES

CMD design and assembly

The blueprint of the microfluidic device was drawn using AUTOCAD (Autodesk, Mill Valley, CA, USA) as two independent sets of channel networks, subsequently printed as high-resolution photomasks (Selba S.A., Versoix, Switzerland). Each photomask was then sequentially used to pattern a layer of photoresistors onto a silicon wafer using SU2020 and SU2100 (MicroChem Corp., Kayaku, Westborough, MA, USA) for 20- and 100-μm deep channels, respectively, as described previously (Bouhedda et al., 2021). The PDMS replica was then obtained by covering the mold with a 5-mm thick layer of 10/1 PDMS base/curing agent mixture (SylGard 184; Dow Corning, Midland, MI, USA). Upon curing, the slab of PDMS was cut off the mold and inlets/outlets were punched using a 1-mm biopsy punch (Harris UniCore, Cytiva, Marlborough-UK). Importantly, the media inlet and the outlet were punched vertically (Figure 1b), whereas the inlet in which the tip containing the seedling has to be inserted was punched at a 45° angle to ensure a smooth entry of the root in the main channel of the device. The piece of PDMS was finally bounded onto a 24 mm $\times$ 60 mm microscope coverslip (VWR, Radnor, PA, USA) by activating both surfaces with an oxygen plasma (Femto; Diener, Ebhausen, Germany) prior to placing them in contact and baking the montage for 10 min at 65°C. Finally, channel surface was passivated by flushing a 1% solution of 1H,1H,2H,2H-perfluorodecyltrichlorosilane 97% stabilized with Copper (ABCR, Karlsruhe, Germany) prepared in Novec 7500 fluorinated oil (3M, Saint Paul, MN, USA) and later flushed off the chip using compressed air.

Plant material and growth conditions

We used seeds of *Arabidopsis thaliana* plants expressing *pSUN1:SUN1-GFP* (Graumann et al., 2010) and *pSUN2:SUN2-RFP-35S:GFP-MBD* after crossing the *pSUN2:SUN2-RFP* (Tamura et al., 2013) and *35S:GFP-MBD lines* (Camilleri et al., 2002) in a Columbia (Col-0) background. After sterilization, seeds were transferred into 200-μl micropipette tips (cut 4 mm in height from the base) already filled with 10 μl of ½ MS medium (SERVA Electrophoresis, Heidelberg, Germany) containing 0.5% sucrose and 1.0% agar. After stratification at 4°C for 48 h in dark, seedling were grown *in vitro* on ½ MS in the presence of 0.5% sucrose and 1.0% agar under long day conditions (16 h of light with 70 μmol m^{-2} per second of fluorescent lighting/8 h of dark at 23°C for 4–5 days (Figure S1c). Afterwards, tips with growing seedlings were transferred into the microfluidic device and placed in the growth chamber for 4–5 days under a constant flow rate of medium

(8 μl min^{-1}) supplied by a pump (Fusion 200; Chemyx, Stafford, TX, USA) connected to the device. To label the cell wall, propidium iodide was used (1 μg ml^{-1}).

Confocal image acquisition and analysis

Confocal images were recorded with a LSM 700 confocal microscope (Zeiss, Wetzlar, Germany) equipped with 10 × 0.3, 20 × 0.8 and oil 40 × 1.3 lens objectives. For analysis of RH growth and nuclear dynamics, the PDMS device was maintained under a continuous flow of liquid media to minimize evaporation during scanning. GFP were imaged with excitation at 488 nm and emission at 510 nm, respectively. For propidium iodide, and RFP imaging, the excitation and emission wavelengths were 555 and 617 nm, respectively. Imaging was performed using Z-stack ranking from 1.0 to 4 μm during time lapse ranking from 10 to 60 min. Observations were performed in multitracking mode using 488- and 555-nm laser excitation. Quantification analysis was performed using IMAGEJ (NIH, Bethesda, MD, USA).

Statistical analysis

For each distribution with $n < 30$ cells, an Anderson–Darling test was performed to investigate the normality of the distributions. For normal distributions or distributions with $n \geq 30$ cells, a Levene's test was performed to investigate the equality of the variance, and then a *t*-test was performed using the result of Levene's test as a parameter (equal or unequal variance).

ACKNOWLEDGEMENTS

This work was supported by the Centre National de la Recherche Scientifique (CNRS) and by HFSP grant 2018, RGP, 009. The study was partially supported by the labex 'Who AM I?', labex ANR-11-LABX- 0071, as well as the Université de Paris, Idex ANR-18- IDEX-0001, funded by the French Government through its 'Investments for the Future' program. This work was partially supported by the Interdisciplinary Thematic Institute 'IMCBio' (to MR), as part of the ITI 2021-2028 program of the University of Strasbourg, CNRS and Inserm, by IdEx Unistra (ANR-10-IDEX-0002), and by SFRI-STRAT'US project and EUR IMCBio (ANR-17-EURE-0023) under the framework of the French Investments for the Future Program. It was also supported by the Centre National de la Recherche Scientifique and the Université de Strasbourg from whom MR received support via its Initiative of Excellence (IdEx). We thank J. Mutterer for help with the confocal imaging, as well as K. Graumann and K. Tamura for providing SUN nuclear envelope marker lines.

CONFLICT OF INTEREST

The authors declare no conflict of interest.

AUTHOR CONTRIBUTIONS

MEC, AA and GS designed the experiments; MR and SB designed and prepared the microfluidic devices; GS and EH performed the experiments; GS, MEC and DP analyzed the data; GS and DP prepared the figures; AA, GS, DP and MEC wrote the paper.

DATA AVAILABILITY STATEMENT

All relevant data are contained within the published article and its supporting materials.

SUPPORTING INFORMATION

Additional Supporting Information may be found in the online version of this article.

Figure S1. (a, b) Detail measurement of the chip indicating the main channel with 90 degree-oriented side channels. (c) 5 days-old Arabidopsis seedlings grown into micro pipette tips containing ½ MS media supplemented with 0.5% sugar and 1% agar.

Figure S2. (a) Image of the microfluidic chip filled with xylene blue. The yellow line represents the line used to do the kymograph of figure (b) below. (b) Kymograph extracted from the Movie S1. Each vertical line reports the color time evolution inside a given lateral channel, and thus to what extent it is filled at a given time. After 29 sec, one can consider that the lateral channels are fully filled with xylene blue since there is no noticeable changes in the color below the horizontal line at 29 sec. Please note that the appearance of such horizontal lines indicate that lateral channels are filled simultaneously all along the chip. Scale bar 400 μm.

Figure S3. Real-time position of the nucleus from the growing RH tip. The nuclear distance from the growing RH tip remains more or less constant. Measurement of the nuclear distance from the *pSUN2:SUN2-RFP* Arabidopsis RH tip for individual nuclei at each minute during 10 min. Confocal images were analyzed with maximal Z-stack projections ($n = 5$).

Figure S4. Instantaneous velocity of the nucleus (yellow) and the RH tip (black). Over long time scales, the instantaneous speed of the nucleus may display fluctuations, although its values are always centred around the rate at which the RH tip is growing. This implies that the mean speeds of the nucleus and RH tip are approximately equal and that, during growth, the nucleus is located at a fixed distance from the RH tip, even though it displays fluctuations around its mean position. Images were acquired every 10 min with a 20× objective.

Figure S5. Shape change analysis of the growing RH nuclei in real time. Measurement of change in aspect ratio, area, perimeter and circularity of 12 individual RH nuclei. Ten minutes of imaging was performed with 1 min/Z-stack ($n = 12$).

Movie S1. Real-time video (1.46 min) showing complete filling of the device with xylene blue at a flow rate of 1000 μl min^{-1}. Scale bar = 400 μm.

Movie S2. Video (60 min) showing RH tip expansion inside the CMD chip (propidium iodide in red; scale bar = 50 μm) (5 fps video).

Movie S3. Video (26 min) showing nuclear movement in growing RH expressing the nuclear envelope marker *pSUN2:SUN2-RFP* into the CMD chip (scale bar = 10 μm) (5 fps video).

Movie S4. Video (43 min) showing high speed nuclear movement inside the mature RH expressing the nuclear envelope marker *pSUN1:SUN1-GFP* (propidium iodide in red; scale bar = 10 μm) (5 fps video).

REFERENCES

Agudelo, C.G., Sanati, A., Ghanbari, M., Packirisamy, M. & Geitmann, A. (2012) A microfluidic platform for the investigation of elongation growth in pollen tubes. *Journal of Micromechanics and Microengineering*, **22**, 115009. https://doi.org/10.1088/0960-1317/22/11/115009

Almonacid, M., Jord, A.A., El Hayek, S., Othmani, A., Coulpier, F., Lemoine, S. *et al.* (2019) Active fluctuations of the nuclear envelope shape the transcriptional dynamics in oocytes. *Developmental Cell*, **51**, 147–157.

Aufrecht, J.A., Ryan, J.M., Hasim, S., Allison, D.P., Nebenführ, A., Doktycz, M.J. *et al.* (2017) Imaging the root hair morphology of *Arabidopsis*

seedlings in a two-layer microfluidic platform. *Journal of Visualized Experiments: Jove*, **126**. https://doi.org/10.3791/55971

Balakrishnan, S., Raju, S.R., Barua, A. & Ananthasuresh, G.K. (2020) Predicting the tension in actin cytoskeleton from the nucleus shape. *bioRxiv*. https://www.biorxiv.org/content/early/2020/08/29/2020.08.28.272435

Bouhedda, F., Cubi, R., Baudrey, S. & Ryckelynck, M. (2021) μIVC-Seq: a method for ultrahigh-throughput development and functional characterization of small RNAs. *Methods in Molecular Biology*, **2300**, 203–237.

Brechenmacher, L., Nguyen, T.H.N., Hixson, K., Libault, M., Aldrich, J., Pasa Tolic, L. *et al.* (2012) Identification of soybean proteins from a single cell type: the root hair. *Proteomics*, **12**, 3365–3373.

Brochhausen, L., Maisch, J. & Nick, P. (2016) Break of symmetry in regenerating tobacco protoplasts is independent of nuclear positioning. *Journal of Integrative Plant Biology*, **58**, 799–812.

Busch, W., Moore, B.T., Martsberger, B., Mace, D.L., Twigg, R.W., Jung, J. *et al.* (2012) A microfluidic device and computational platform for high-throughput live imaging of gene expression. *Nature Methods*, **9**, 1101–1106.

Camilleri, C., Azimzadeh, J., Pastuglia, M., Bellini, C., Grandjean, O. & Bouchez, D. (2002) The *Arabidopsis TONNEAU2* gene encodes a putative novel protein phosphatase 2A regulatory subunit essential for the control of the cortical cytoskeleton. *The Plant Cell*, **14**, 833–845.

Chu, F.Y., Haley, S.C. & Zidovska, A. (2017) On the origin of shape fluctuations of the cell nucleus. *Proceedings of the National Academy of Sciences of the United States of America*, **114**, 10338–10343.

Chytilova, E., Macas, J., Sliwinska, E., Rafelski, S.M., Lambert, G.M. & Galbraith, D.W. (2000) Nuclear dynamics in *Arabidopsis thaliana*. *Molecular Biology of the Cell*, **11**, 2733–2741.

Dolan, L., Duckett, C.M., Grierson, C., Linstead, P., Schneider, K., Lawson, E. *et al.* (1994) Clonal relationships and cell patterning in the root epidermis of Arabidopsis. *Development*, **120**, 2465–2474.

Dorland, Y.L., Cornelissen, A.S., Kuijk, C., Tol, S., Hoogenboezem, M., van Buul, J.D. *et al.* (2019) Nuclear shape, protrusive behaviour and in vivo retention of human bone marrow mesenchymal stromal cells is controlled by Lamin-A/C expression. *Scientific Reports*, **9**, 1–15.

Fal, K., Korsbo, N., Alonso-Serra, J., Teles, J., Liu, M., Refahi, Y. *et al.* (2021) Tissue folding at the organ-meristem boundary results in nuclear compression and chromatin compaction. *Proceedings of the National Academy of Sciences USA*, **118**. https://doi.org/10.1073/pnas.2017859118

Fendrych, M., Akhmanova, M., Merrin, J., Glanc, M., Hagihara, S., Takahashi, K. *et al.* (2018) Rapid and reversible root growth inhibition by TIR1 auxin signalling. *Nature Plants*, **4**, 453–459.

Goswami, R., Asnacios, A., Hamant, O. & Chabouté, M.E. (2020) Is the plant nucleus a mechanical rheostat? *Current Opinion in Plant Biology*, **57**, 155–163. https://doi.org/10.1016/j.pbi.2020.09.001

Goswami, R., Asnacios, A., Milani, P., Graindorge, S., Houlné, G., Mutterer, J. *et al.* (2020) Mechanical shielding in plant nuclei. *Current Biology*, **30**, 2013–2025.

Goto, C., Tamura, K., Nishimaki, S., Maruyama, D. & Hara-Nishimura, I. (2020) The nuclear envelope protein KAKU4 determines the migration order of the vegetative nucleus and sperm cells in pollen tubes. *Journal of Experimental Botany*, **71**, 6273–6281.

Graumann, K., Runions, J. & Evans, D.E. (2010) Characterization of SUN-domain proteins at the higher plant nuclear envelope. *The Plant Journal*, **61**, 134–144.

Grierson, C., Nielsen, E., Ketelaarc, T. & Schiefelbein, J. (2014) Root hairs. *The Arabidopsis Book, American Society of Plant Biologists*, **12**, 1–25. https://doi.org/10.1199/tab.0172

Griffis, A.H.N., Groves, N.R., Zhou, X. & Meier, I. (2014) Nuclei in motion: movement and positioning of plant nuclei in development, signaling, symbiosis, and disease. *Frontiers in Plant Science*, **5**, 1–7.

Guichard, M., Garcia, B., de Olalla, E., Stanley, C.E. & Grossmann, G. (2020) Microfluidic systems for plant root imaging. *Methods in Cell Biology*, **160**, 381–404.

Hepler, P.K., Vidali, L. & Cheung, A.Y. (2001) Polarized cell growth in higher plants. *Annual Review of Cell and Developmental Biology*, **17**, 159–187.

Jiang, H., Xu, Z., Aluru, M.R. & Dong, L. (2014) Plant chip for high-throughput phenotyping of Arabidopsis. *Lab on a chip*, **14**, 1281–1293.

Jones, M.A., Shen, J.-J., Fu, Y., Li, H., Yang, Z. & Grierson, C.S. (2002) The *Arabidopsis* Rop2 GTPase is a positive regulator of both root hair initiation and tip growth. *The Plant Cell*, **14**, 763–776.

Kang, E., Zheng, M., Zhang, Y., Yuan, M., Yalovsky, S., Zhu, L. *et al.* (2017) The microtubule-associated protein MAP18 affects ROP2 GTPase activity during root hair growth. *Plant Physiology*, **174**, 202–222.

Ketelaar, T., Faivre-Moskalenko, C., Esseling, J.J., Ruijter, N.C.A.D., Grierson, C.S., Dogterom, M. *et al.* (2002) Positioning of nuclei in *Arabidopsis* root hairs: an actin-regulated process of tip growth. *The Plant Cell*, **14**, 2941–2955.

Krupinski, P., Bozorg, B., Larsson, A., Pietra, S., Grebe, M. & Jönsson, H. (2016) A model analysis of mechanisms for radial microtubular patterns at root hair initiation sites. *Frontiers in Plant Science*, **7**, https://doi.org/10.3389/fpls.2016.01560

Lan, P., Li, W., Lin, W.D., Santi, S. & Schmidt, W. (2013) Mapping gene activity of *Arabidopsis* root hairs. *Genome Biology*, **14**(R67), 1–20.

Landrein, B., Kiss, A., Sassi, M., Chauvet, A., Das, P., Cortizo, M. *et al.* (2015) Mechanical stress contributes to the expression of the STM homeobox gene in *Arabidopsis* shoot meristems. *Elife*, **4**, e07811.

Li, W. & Lan, P. (2015) Re-analysis of RNA-seq transcriptome data reveals new aspects of gene activity in *Arabidopsis* root hairs. *Frontiers in Plant Science*, **6**, 421.

Libault, M., Farmer, A., Brechenmacher, L., Drnevich, J., Langley, R.J., Bilgin, D.D. *et al.* (2010) Complete transcriptome of the soybean root hair cell, a single-cell model, and its alteration in response to *Bradyrhizobium japonicum* infection. *Plant Physiology*, **152**, 541–552.

Lockhart, J.A. (1965) An analysis of irreversible plant cell elongation. *Journal of Theoretical Biology*, **8**, 264–275.

Massalha, H., Korenblum, E., Malitsky, S., Shapiro, O.H. & Aharoni, A. (2017) Live imaging of root-bacteria interactions in a microfluidics setup. *Proceedings of the National Academy of Sciences of the United States of America*, **114**, 4549–4554.

Meier, I., Griffis, A.H., Groves, N.R. & Wagner, A. (2016) Regulation of nuclear shape and size in plants. *Current Opinion in Cell Biology*, **40**, 114–123.

Misra, C.S., Santos, M.R., Rafael-Fernandes, M., Martins, N.P., Monteiro, M. & Becker, J.D. (2019) Transcriptomics of *Arabidopsis* sperm cells at single-cell resolution. *Plant Reproduction*, **32**, 29–38.

Newman-Griffis, A.H., del Cerro, P., Charpentier, M. & Meier, I. (2019) *Medicago* LINC complexes function in nuclear morphology, nuclear movement, and root nodule symbiosis. *Plant Physiology*, **179**, 491–506.

Parashar, A. & Pandey, S. (2011) Plant-in-chip: microfluidic system for studying root growth and pathogenic interactions in *Arabidopsis*. *Applied Physics Letters*, **98**, https://doi.org/10.1063/1.3604788

Petricka, J.J., Schauer, M.A., Megraw, M., Breakfield, N.W., Thompson, J.W., Georgiev, S. *et al.* (2012) The protein expression landscape of the *Arabidopsis* root. *Proceedings of the National Academy of Sciences of the United States of America*, **109**, 6811–6818.

Qiao, Z., Pingault, L., Zogli, P., Langevin, M., Rech, N., Farmer, A. *et al.* (2017) A comparative genomic and transcriptomic analysis at the level of isolated root hair cells reveals new conserved root hair regulatory elements. *Plant Molecular Biology*, **94**, 641–655.

Ryu, K.H., Huang, L., Kang, H.M. & Schiefelbein, J. (2019) Single-cell RNA sequencing resolves molecular relationships among individual plant cells. *Plant Physiology*, **179**, 1444–1456.

Satterlee, J.W., Strable, J. & Scanlon, M.J. (2021) Plant stem-cell organization and differentiation at single-cell resolution. *Proceedings of the National Academy of Sciences of the United States of America*, **117**, 33689–33699.

Shibata, M., Breuer, C., Kawamura, A., Clark, N.M., Rymen, B., Braidwood, L. *et al.* (2018) *GTL1* and *DF1* regulate root hair growth through transcriptional repression of ROOT HAIR DEFECTIVE 6-LIKE 4 in *Arabidopsis*. *Development*, **145**, https://doi.org/10.1242/dev.159707

Sieberer, B.J., Ketelaar, T., Esseling, J.J. & Emons, A.M.C. (2005) Microtubules guide root hair tip growth. *New Phytologist*, **167**, 711–719.

Stanley, C.E., Shrivastava, J., Brugman, R., Heinzelmann, E., van Swaay, D. & Grossmann, G. (2018) Dual-flow-RootChip reveals local adaptations of roots towards environmental asymmetry at the physiological and genetic levels. *New Phytologist*, **217**, 1357–1369.

Sun, L., Liu, L., Lin, X., Xia, Z., Cao, J., Xu, S. *et al.* (2021) Microfluidic devices for monitoring the root morphology of *Arabidopsis thaliana* in situ. *Analytical Sciences*, **37**, 605–611.

Tamura, K., Iwabuchi, K., Fukao, Y., Kondo, M., Okamoto, K., Ueda, H. *et al.* (2013) Myosin XI-i links the nuclear membrane to the cytoskeleton to control nuclear movement and shape in Arabidopsis. *Current Biology*, **23**, 1776–1781.

Van Bruaene, N., Joss, G., Thas, O. & Van Oostveldt, P. (2003) Four-dimensional imaging and computer-assisted track analysis of nuclear migration in root hairs of *Arabidopsis thaliana*. *Journal of Microscopy*, **211**, 167–178.

Van Bruaene, N., Joss, G. & Van Oostveldt, P. (2004) Reorganization and *in vivo* dynamics of microtubules during *Arabidopsis* root hair development. *Plant Physiology*, **136**, 3905–3919.

Vassileva, V.N., Kouchi, H. & Ridge, R.W. (2005) Microtubule dynamics in living root hairs: transient slowing by lipochitin oligosaccharide nodulation signals. *The Plant Cell*, **17**, 1777–1787.

Versaevel, M., Grevesse, T. & Gabriele, S. (2012) Spatial coordination between cell and nuclear shape within micropatterned endothelial cells. *Nature Communications*, **14**, 1–11.

Volgger, M., Lang, I., Ovecka, M. & Lichtscheidl, I. (2010) Plasmolysis and cell wall deposition in wheat root hairs under osmotic stress. *Protoplasma*, **243**, 51–62.

Wymer, C.L., Bibikova, T.N. & Gilroy, S. (1997) Cytoplasmic free calcium distributions during the development of root hairs of *Arabidopsis thaliana*. *The Plant Journal*, **12**, 427–439.

Yamada, M. & Goshima, G. (2018) The KCH kinesin drives nuclear transport and cytoskeletal coalescence to promote tip cell growth in *Physcomitrella patens*. *The Plant Cell*, **30**, 1496–1510.

Yi, K., Menand, B., Bell, E. & Dolan, L. (2010) A basic helix-loop-helix transcription factor controls cell growth and size in root hairs. *Nature Genetics*, **42**, 264–267.

Zhang, S., Liu, J., Xue, X., Tan, K., Wang, C. & Su, H. (2019) The migration direction of hair cell nuclei is closely related to the perinuclear actin filaments in *Arabidopsis*. *Biochemical and Biophysical Research Communications*, **519**, 783–789.